Domain and Subband decomposition approach for 2D simulation of quantum transport phenomena*

Hao Wu†

In the memory of Naoufel Ben Abdallah

May 12, 2011

Abstract

We present a domain decomposition technical for computing the quantum transport phenomena in complex nano-structures. In regular sub-domains, the subband decomposition method is applied, while the finite difference method is used on small irregular sub-domains where the subband decomposition is not applicable. This new approach preserves the efficiency of the original subband decomposition method, with a minor increase of the computational cost. Results of numerical experiments demonstrate the efficiency and accuracy of this method.

Key words. Schrödinger equation, domain decomposition, subband decomposition, confined boundary condition, semiclassical regime.

1 Introduction

The main purpose of this paper is to extend the efficient subband decomposition method for the 2D Schrödinger equation on the complicated computational domain $\Omega \subset \mathbb{R}^2$:

$$-\frac{1}{2}\varepsilon^2 \left(\partial_{xx} + \partial_{yy}\right)\varphi + V\varphi = E\varphi, \quad (x, y) \in \Omega, \tag{1.1}$$

with specific boundary conditions, where ε is the re-scaled Planck constant, E is the specified energy, $\varphi = \varphi(x, y)$ denotes the wave function, and $V = V(x, y)$ is the smooth external potential.

A typical complicated computational domain Ω is shown in Figure 1. This is a 2D simplified model of the full dimensional quantum directional coupler [18, 19, 20]. The boundary conditions are given as

*This work was partially supported by the ANR Project No. BLAN07-2 212988 entitled "QUATRAIN", NSFC Projects 11071139 and NSFC Projects 10971115.

†Department of Mathematical Sciences, Tsinghua University, Beijing, 10084, China(hwu@tsinghua.edu.cn)

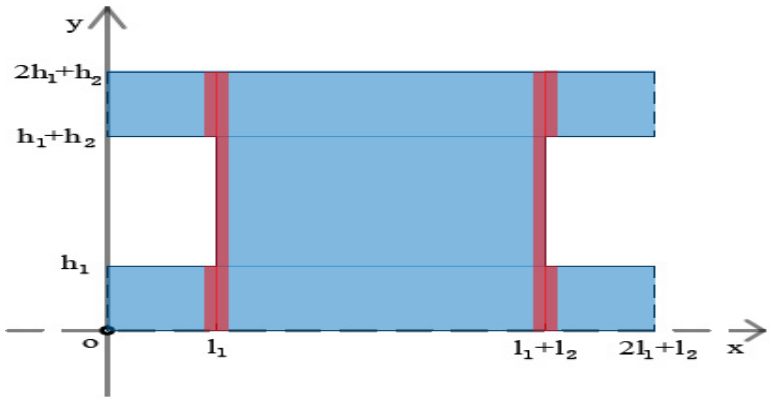

Figure 1: The computational domain and the graphic interpretation of the domain decomposition method.

- On $(x,y) \in \Gamma_c = \cup_{p=1}^{8} \Gamma_c^p$, the confined boundary conditions are used,

$$\varphi(x,y)|_{(x,y)\in\Gamma_c} = 0,$$

which prevent electrons from leaving out of the computational domain. For practical semiconductor devices, they are usually made up of insulators. Therefore, electrons are located inside the device. Here we have

$$\Gamma_c^1 = \left\{(x,0)\middle|0 \le x \le 2l_1 + l_2\right\},\ \Gamma_c^2 = \left\{(x,2h_1+h_2)\middle|0 \le x \le 2l_1 + l_2\right\},$$
$$\Gamma_c^3 = \left\{(x,h_1)\middle|0 \le x \le l_1\right\},\ \Gamma_c^4 = \left\{(x,h_1+h_2)\middle|0 \le x \le l_1\right\},$$
$$\Gamma_c^5 = \left\{(x,h_1)\middle|l_1 + l_2 \le x \le 2l_1 + l_2\right\},\ \Gamma_c^6 = \left\{(x,h_1+h_2)\middle|l_1 + l_2 \le x \le 2l_1 + l_2\right\},$$
$$\Gamma_c^7 = \left\{(l_1,y)\middle|h_1 \le y \le h_1 + h_2\right\},\ \Gamma_c^8 = \left\{(l_1+l_2,y)\middle|h_1 \le y \le h_1 + h_2\right\}.$$

- On $(x,y) \in \Gamma_t = \cup_{p=1}^{4} \Gamma_t^p$, the transparent boundary conditions are used[1], which allow electrons move in and out of the computational domain. In practical semiconductor devices, they are usually connected to highly conducting reservoirs. Therefore, electrons can be exchanged with the external electrical circuit. Here we have

$$\Gamma_t^1 = \left\{(0,y)\middle|0 \le y \le h_1\right\},\ \Gamma_t^2 = \left\{(0,y)\middle|h_1 + h_2 \le y \le 2h_1 + h_2\right\},$$
$$\Gamma_t^3 = \left\{(2l_1+l_2,y)\middle|0 \le y \le h_1\right\},\ \Gamma_t^4 = \left\{(2l_1+l_2,y)\middle|h_1 + h_2 \le y \le 2h_1 + h_2\right\}.$$

The quantum directional couplers were firstly proposed by Alamo and Eugster [4, 11]. Such devices are designed to construct new electron transport modes, because the transport properties are significantly determined by the

[1]We will present the formulas in the later sections.

devices' geometry. Based on this principle, different structures, e.g., T-stub [7, 23], Y-branch [17], rings [8] and crosses [22] have been proposed. For these devices, the computational domains are complicated in the numerical simulations.

In these devices, quantum effect is important since the length scale is very small. Therefore, the oscillatory properties of the wave functions induce serious numerical difficulties for direct methods [14]. The $o(\varepsilon)$ mesh size is required for the finite difference method [25, 26]. The spectral type method [5, 6] could relax the mesh size requirement to be $O(\varepsilon)$. But this method, to the author's knowledge, cannot be easily applied when the simulations are performed on complicated computational domain.

The subband decomposition method [2, 18, 19] is an alternative numerical method. In view of the strong confinement of electrons in the devices, we can split a higher dimensional Schrödinger equation into one lower dimensional Schrödinger equation in the confined direction and the other lower dimensional Schrödinger equation in the transport direction. This idea may fail here, because the link mode for different subbands at $x = l_1$ or $x = l_1+l_2$ in Figure 1 is not clearly known.

In this paper, we develop a domain decomposition approach to deal with the aforementioned difficulty. The general idea of domain decomposition is to split the original problem into coupled problems on small sub-domains. There are three levels of domain decomposition, which are the continuous level [9, 10, 12, 15], the discretization level [3, 13, 21] and the algebraic level [24, 27, 28]. They are also categorized into the overlapping decomposition [3, 9, 10, 13, 27] and the non-overlapping decomposition [12, 15, 21, 28].

We will concern the non-overlapping decomposition on the discretization level. In regular sub-domains, the subband decomposition method will be applied to reduce the computational cost. And the finite difference method will be used in irregular sub-domains. The two sub-domains are coupled by proper interface conditions. Compare to the original subband decomposition method, the increasing of algorithm complexity is minor because irregular sub-domains are small.

This paper is organized as follows. In Section 2, the domain decomposition based subband decomposition and the finite difference method is designed. The two kinds of discrete interface conditions are proposed in Subsection 2.2 and Subsection 2.3 respectively. Numerical examples are given in Section 3 to test the efficiency and accuracy. We make some conclusive remarks in Section 4.

2 The domain decomposition approach

To compute the wave function $\varphi(x, y)$ for the stationary Schrödinger equation (1.1) with specific boundary conditions numerically, we firstly decom-

pose the computational domain Ω into the finite difference domain Ω_d and the subband decomposition domain Ω_s:

- The finite difference domain, which corresponds to the red part in Figure 1, is made up of six sub-domains

$$\Omega_d = \cup_{p=1}^{6} \Omega_d^p,$$

where

$$\begin{aligned}
\Omega_d^1 &= \left\{(x,y)\middle| l_1 - \delta \le x \le l_1,\ 0 \le y \le h_1\right\}, \\
\Omega_d^2 &= \left\{(x,y)\middle| l_1 - \delta \le x \le l_1,\ h_1 + h_2 \le y \le 2h_1 + h_2\right\}, \\
\Omega_d^3 &= \left\{(x,y)\middle| l_1 \le x \le l_1 + \delta,\ 0 \le y \le 2h_1 + h_2\right\}, \\
\Omega_d^4 &= \left\{(x,y)\middle| l_1 + l_2 - \delta \le x \le l_1 + l_2,\ 0 \le y \le 2h_1 + h_2\right\}, \\
\Omega_d^5 &= \left\{(x,y)\middle| l_1 + l_2 \le x \le l_1 + l_2 + \delta,\ 0 \le y \le h_1\right\}, \\
\Omega_d^6 &= \left\{(x,y)\middle| l_1 + l_2 \le x \le l_1 + l_2 + \delta,\ h_1 + h_2 \le y \le 2h_1 + h_2\right\}.
\end{aligned}$$

Here δ is the small positive interval length.

- The subband decomposition domain, which corresponds to the blue part in Figure 1, is made up of five sub-domains

$$\Omega_s = \cup_{p=1}^{5} \Omega_s^p,$$

where

$$\begin{aligned}
\Omega_s^1 &= L_x^1 \times L_y^1, \quad L_x^1 = [0, l_1 - \delta],\ L_y^1 = [0, h_1], \\
\Omega_s^2 &= L_x^2 \times L_y^2, \quad L_x^2 = L_x^1,\ L_y^2 = [h_1 + h_2, 2h_1 + h_2], \\
\Omega_s^3 &= L_x^3 \times L_y^3, \quad L_x^3 = [l_1 + l_2 + \delta, 2l_1 + l_2],\ L_y^3 = L_y^1, \\
\Omega_s^4 &= L_x^4 \times L_y^4, \quad L_x^4 = L_x^3,\ L_y^4 = L_y^2, \\
\Omega_s^5 &= L_x^5 \times L_y^5, \quad L_x^5 = [l_1 + \delta, l_1 + l_2 - \delta],\ L_y^5 = [0, 2h_1 + h_2].
\end{aligned}$$

In the finite difference domain Ω_d, the central difference approximation can be used for (1.1):

$$-\frac{\varepsilon^2}{2h^2}\left(\varphi^{i-1,j} + \varphi^{i+1,j} + \varphi^{i,j-1} + \varphi^{i,j+1} - 4\varphi^{i,j}\right) + V^{i,j}\varphi^{i,j} = E\varphi^{i,j}, \quad (2.1)$$

with $\varphi^{i,j} = \varphi(x_i, y_j)$, (x_i, y_j) denotes the grid point, and $\Delta x = \Delta y = h$ gives the mesh size.

In the subband decomposition domain Ω_s, the wave function $\varphi(x,y)$ is expanded into series of multi-mode bases $\chi_n^p(x,y)$:

$$\varphi(x,y) = \sum_{n=1}^{\infty} \phi_n^p(x)\chi_n^p(x,y) \approx \sum_{n=1}^{N_p} \phi_n^p(x)\chi_n^p(x,y),\ \forall (x,y) \in \Omega_s^p, \quad (2.2)$$

with

$$\phi_n^p(x) = \int_{L_y^p} \varphi(x,y)\overline{\chi}_n^p(x,y)\mathrm{d}y.$$

Here $(E_n^p(x), \chi_n^p(x,y))$ are solutions of the eigenvalue problem

$$\begin{cases} -\frac{1}{2}\varepsilon^2\partial_{yy}\chi_n^p(x,y) + V(x,y)\chi_n^p(x,y) = E_n^p(x)\chi_n^p(x,y), \\ \int_{L_y^p}\chi_n^p(x,y)\overline{\chi}_m^p(x,y)\mathrm{d}y = \delta_{n,m}, \quad \chi_n^p(x,y)|_{y\in\partial L_y^p} = 0. \end{cases} \tag{2.3}$$

Then we have the coupled Schrödinger system for $\phi_n^p(x)$

$$-\partial_{xx}\phi_n^p - 2\sum_{m=1}^{N_p} c_{nm}^{p1}\partial_x\phi_m^p - \sum_{m=1}^{N_p} c_{nm}^{p2}\phi_m^p = \frac{2}{\varepsilon^2}(E - E_n^p)\phi_n^p, \tag{2.4}$$

where

$$\begin{aligned} c_{nm}^{p1}(x) &= \int_{L_y^p} \overline{\chi}_n^p(x,y)\partial_x\chi_m^p(x,y)\mathrm{d}y, \\ c_{nm}^{p2}(x) &= \int_{L_y^p} \overline{\chi}_n^p(x,y)\partial_{xx}\chi_m^p(x,y)\mathrm{d}y. \end{aligned}$$

It is easy to check that

$$c_{nn}^{p1}(x) = c_{nn}^{p2}(x) = 0.$$

The equations (2.4) can be discretized in the central difference form

$$-\frac{\phi_n^{p,i+1} - 2\phi_n^{p,i} + \phi_n^{p,i-1}}{h^2} - \sum_{m=1}^{N_p} c_{nm}^{p1,i}\frac{\phi_m^{p,i+1} - \phi_m^{p,i-1}}{h} - \sum_{m=1}^{N_p} c_{nm}^{p2,i}\phi_m^{p,i} = \frac{2}{\varepsilon^2}\left(E - E_n^{p,i}\right)\phi_n^{p,i}, \tag{2.5}$$

with $\phi_n^{p,i} = \phi_n^p(x_i)$ and $c_{nm}^{p,s,i} = c_{nm}^{ps}(x_i)$.

Remark 2.1 *In* (2.2)*, N_p denotes the number of subbands used for approximating $\varphi(x,y)$ in sub-domain Ω_s^p. Let M_p be the number of y-direction grid points in the same sub-domain. If $N_p \ll M_p$, which is true in practical simulations, the subband decomposition method can save a lot of computational resources compare with the finite difference method*

Remark 2.2 *In practical simulations, we can use the r-coupling modes model to reduce the number of non-zero elements in the matrix form of* (2.5)*, i.e., $c_{nm}^{p1}(x)$ and $c_{nm}^{p2}(x)$ are set to zero for $|m-n| > r$. This r-coupling modes may give convergent numerical results when $r \geq 2$. The detailed discussions can be found in [19].*

2.1 The transparent boundary condition

In this subsection, we remind the transparent boundary condition for Γ_t. The detailed derivations can be found in [1, 16]. For $p = 1, 2$, the boundary conditions on Γ_t^p are

$$\varepsilon\partial_x\varphi(0,y) = \sum_{E>E_n^p} i\sqrt{2(E-E_n^p)}\,(2a_n^p - \phi_n^p(0))\,\chi_n^p(0,y) + \sum_{E\le E_n^p} \sqrt{2(E_n^p-E)}\phi_n^p(0)\chi_n^p(0,y),\ \forall(0,y)\in\Gamma_t^p. \quad (2.6)$$

For $p = 3, 4$, the boundary conditions on Γ_t^p are

$$\varepsilon\partial_x\varphi(2l_1+l_2,y) = \sum_{E>E_n^p} i\sqrt{2(E-E_n^p)}\,(\phi_n^p(2l_1+l_2) - 2a_n^p)\,\chi_n^p(2l_1+l_2,y) - \sum_{E\le E_n^p} \sqrt{2(E_n^p-E)}\phi_n^p(2l_1+l_2)\chi_n^p(2l_1+l_2,y),\ \forall(0,2l_1+l_2)\in\Gamma_t^p. \quad (2.7)$$

Here a_n^p are the coefficients of incoming waves. Writing (2.6)-(2.7) into discrete form, we have

$$\frac{\varepsilon}{h}\left(-\frac{3}{2}\phi_n^{p,1} + 2\phi_n^{p,2} - \frac{1}{2}\phi_n^{p,3}\right) = \begin{cases} i\sqrt{2(E-E_n^p)}\left(2a_n^p - \phi_n^{p,1}\right), & E > E_n^p, \\ \sqrt{2(E_n^p-E)}\phi_n^{p,1}, & E \le E_n^p, \end{cases} \quad (2.8)$$

and

$$\frac{\varepsilon}{h}\left(\frac{3}{2}\phi_n^{p,I} - 2\phi_n^{p,I-1} + \frac{1}{2}\phi_n^{p,I-2}\right) = \begin{cases} i\sqrt{2(E-E_n^p)}\left(\phi_n^{p,I} - 2a_n^p\right), & E > E_n^p, \\ -\sqrt{2(E_n^p-E)}\phi_n^{p,I}, & E \le E_n^p. \end{cases} \quad (2.9)$$

2.2 The discrete interface conditions A

Now we derive the discrete interface conditions that connect the finite difference method and the subband decomposition method. Without loss of generality, we only consider the interface

$$\Gamma_i^1 = \left\{(l_1-\delta, y)\middle| 0 \le y \le h_1\right\}.$$

Let

$$x_{L_1} = l_1 - \delta, \quad y_1 = 0, \quad y_{J_1} = h_1,$$

then the stationary Schrödinger equation (1.1) can be discretized as

$$-\sum_{n=1}^{N_1}\phi_n^{1,L_1-1}\chi_n^{1,L_1-1,j}-\varphi^{L_1+1,j}-\varphi^{L_1,j-1}-\varphi^{L_1,j+1} + \left(4-\frac{2h^2}{\varepsilon^2}\left(E-V^{L_1,j}\right)\right)\varphi^{L_1,j}=0. \quad (2.10)$$

with

$$\chi_n^{p,i,j}=\chi_n^p(x_i,y_j).$$

On the other hand, the coupled stationary Schrödinger equation system (2.4) can be discretized as

$$-h\sum_{j=1}^{J_1}\varphi^{L_1,j}\overline{\chi}_n^{1,L_1,j}+2\phi_n^{1,L_1-1}-\phi_n^{1,L_1-2}-h\sum_{m=1}^{N_1}c_{nm}^{1,1,L_1-1}\left(h\sum_{j=1}^{J_1}\varphi^{L_1,j}\overline{\chi}_m^{1,L_1,j}-\phi_m^{1,L_1-2}\right) - h^2\sum_{m=1}^{N_1}c_{nm}^{1,2,L_1-1}\phi_m^{1,L_1-1}=\frac{2h^2}{\varepsilon^2}\left(E-E_n^{1,L_1-1}\right)\phi_n^{1,L_1-1},$$

which can be reformulated by

$$-h\sum_{j=1}^{J_1}\left(\overline{\chi}_n^{1,L_1,j}+d_n^{1,L_1,j}\right)\varphi^{L_1,j}+\left(\left(2-\frac{2h^2}{\varepsilon^2}E\right)+\frac{2h^2}{\varepsilon^2}E_n^{1,L_1-1}\right)\phi_n^{1,L_1-1} - h^2\sum_{m=1}^{N_1}c_{nm}^{1,2,L_1-1}\phi_m^{1,L_1-1}-\phi_n^{1,L_1-2}+h\sum_{m=1}^{N_1}c_{nm}^{1,1,L_1-1}\phi_m^{1,L_1-2}=0. \quad (2.11)$$

with

$$d_n^{p,i,j}=h\sum_{m=1}^{N_1}c_{nm}^{p,1,i-1}\overline{\chi}_m^{p,i,j}.$$

Writing them into matrix form, we get

$$\begin{pmatrix} -I_{N_1}+hC_{L_1-1}^{1,1} & M_{L_1-1}^1-h^2C_{L_1-1}^{1,2} & -h\left(D_{L_1}^1+\left(X_{L_1}^1\right)^*\right) & \\ & -X_{L_1-1}^1 & P_{L_1} & -I_{J_1}\end{pmatrix}\begin{pmatrix}\widehat{\phi}_{L_1-2}^1\\ \widehat{\phi}_{L_1-1}^1\\ \widehat{\varphi}_{L_1}\\ \widehat{\varphi}_{L_1+1}\end{pmatrix}=0,$$

where

$$\widehat{\phi_i^p}=\left(\phi_1^{p,i},\phi_2^{p,i},\cdots,\phi_{N_1}^{p,i}\right),\quad \widehat{\varphi}_i=\left(\varphi_1^i,\varphi_2^i,\cdots,\varphi_{J_1}^i\right),$$
$$C_i^{p,s}=\left(c_{nm}^{p,s,i}\right)_{N_1\times N_1},\quad D_i^p=\left(d_n^{p,i,j}\right)_{N_1\times J_1},\quad X_i^p=\left(\chi_n^{p,i,j}\right)_{J_1\times N_1}$$

I_n is the $n \times n$ identity matrix,

$$M_i^p = \left(2 - \frac{2h^2}{\varepsilon^2}E\right) + \frac{2h^2}{\varepsilon^2}\begin{pmatrix} E_1^{p,i} & & & \\ & E_2^{p,i} & & \\ & & \ddots & \\ & & & E_{N_1}^{p,i} \end{pmatrix}_{N_1\times N_1},$$

$$P_i = -\frac{2h^2}{\varepsilon^2}E + \begin{pmatrix} 4+\frac{2h^2}{\varepsilon^2}V^{i,1} & -1 & & \\ -1 & 4+\frac{2h^2}{\varepsilon^2}V^{i,2} & \ddots & \\ & \ddots & \ddots & -1 \\ & & -1 & 4+\frac{2h^2}{\varepsilon^2}V^{i,J_1} \end{pmatrix}_{J_1\times J_1}.$$

2.3 The discrete interface conditions B

Similar to Subsection 2.2, we only consider the interface Γ_i^1. We use the fact that the function and its first order normal derivative are continuous, i.e.

$$[\varphi]_{(x,y)} = [\varphi_x]_{(x,y)} = 0, \quad (x,y) \in \Gamma_i^1, \tag{2.12}$$

where $[\cdot]_{(x,y)}$ represents the jump in a quantity at the point (x,y)

$$[\varphi]_{(x,y)} = \varphi^+(x,y) - \varphi^-(x,y).$$

We use superscripts $+$ or $-$ to denote the limiting values of a function from one side (in Ω_d^1) or the other (in Ω_s^1). Then we have the second order discretization of (2.12),

$$\phi_n^{1,L_1} = \sum_{j=1}^{J_1} \varphi^{L_1,j}\overline{\chi}_n^{1,L_1,j}h, \tag{2.13}$$

and

$$\frac{-3\varphi^{L_1,j} + 4\varphi^{L_1+1,j} - \varphi^{L_1+2,j}}{2h} = \sum_n^{N_1}\left(\frac{3\phi_n^{1,L_1} - 4\phi_n^{1,L_1-1} + \phi_n^{1,L_1-2}}{2h}\chi_n^{1,L_1,j} + \phi_n^{1,L_1}\zeta_n^{1,L_1,j}\right), \tag{2.14}$$

with

$$\zeta_n^{p,i,j} = \partial_x\chi_n^p(x_i,y_j).$$

Writing them into matrix form, we get

$$\begin{pmatrix} & & I_{N_1} & -h\left(X_{L_1}^1\right)^* & & \\ \frac{1}{2}X_{L_1}^1 & -2X_{L_1}^1 & \frac{3}{2}X_{L_1}^1 + hY_{L_1}^1 & \frac{3}{2}I_{J_1} & -2I_{J_1} & \frac{1}{2}I_{J_1} \end{pmatrix}\begin{pmatrix} \widehat{\phi}_{L_1-2}^1 \\ \widehat{\phi}_{L_1-1}^1 \\ \widehat{\phi}_{L_1}^1 \\ \widehat{\varphi}_{L_1} \\ \widehat{\varphi}_{L_1+1} \\ \widehat{\varphi}_{L_1+2} \end{pmatrix} = 0,$$

where

$$Y_i^p = \left(\zeta_n^{p,i,j}\right)_{J_1 \times N_1}.$$

3 Numerical examples

In this section, we present several numerical examples to show the accuracy and the efficiency of the numerical scheme. The reference Schrödinger solutions are computed by using the finite difference approximation with a very fine mesh and a very small time step.

Example 1. We consider the two dimensional Schrödinger equation with the following parameters

$$l_1 = h_1 = 0.2,\ l_2 = h_2 = 0.6,\ E = 0.6,\ \varepsilon = 0.05,$$
$$V(x,y) = 0,\ (x,y) \in \Omega,$$
$$a_n^p = \begin{cases} 1, & n = p = 1, \\ 0, & \text{else.} \end{cases}$$

It is easy to see that

$$E_n^p = \begin{cases} \frac{25}{2} n^2 \pi^2 \varepsilon^2, & p = 1,2,3,4, \\ \frac{1}{2} n^2 \pi^2 \varepsilon^2, & p = 5. \end{cases}$$

Therefore, we can believe that

$$N_p = 16\ (p = 1,2,3,4), \quad N_5 = 40,$$

is accurate enough for the subband decomposition method.

For both discrete interface conditions, we output the l^1 errors of wave functions for different mesh sizes h in Table 1. The convergence rate of the errors in h for both discrete interface conditions are about second order. In Figure 2, the contour of the wave amplitude $|\varphi(x,y)|$ is plotted.

We compare the computational time and the l^1 error for the finite difference method and the domain and subband decomposition method in Table 2. From the table, we can see the domain and subband decomposition method is more efficient.

As demonstrated in Figure 3, the error is reduced with increasing the interval length δ. It is because the function is not smooth near $x = l_1$ and $x = l_1 + l_2$, which results a low accuracy of the subband decomposition. On the other hand, the computational cost would increase with larger δ. In this example, we suggest $\delta = 1/80$ as the optimal interval length.

Example 2. We consider the two dimensional Schrödinger equation with the following parameters

$$l_1 = h_1 = 0.2,\ l_2 = h_2 = 0.6,\ E = 1.4,\ \varepsilon = 0.05,$$
$$V(x,y) = 0,\ (x,y) \in \Omega,$$

h	$\frac{1}{100}$	$\frac{1}{200}$	$\frac{1}{400}$	$\frac{1}{800}$
Type A	5.59×10^{-2}	1.29×10^{-2}	2.85×10^{-3}	5.94×10^{-4}
ratio	$---$	4.33	4.53	4.80
Type B	4.39×10^{-2}	1.06×10^{-2}	2.87×10^{-3}	5.66×10^{-4}
ratio	$---$	4.14	3.69	5.07

Table 1: Example 1, the l^1 errors of wave functions for different mesh sizes and discrete interface conditions.

	$h = \frac{1}{400}$		$h = \frac{1}{800}$	
	CPU time	l^1 error	CPU time	l^1 error
Type A	0.69s	2.85×10^{-3}	1.61s	5.94×10^{-4}
Type B	0.93s	2.87×10^{-3}	2.66s	5.66×10^{-4}
Finite difference	4.48s	2.44×10^{-3}	26.05s	5.02×10^{-4}

Table 2: Example 1, comparisons of the domain and subband decomposition method and the finite difference method.

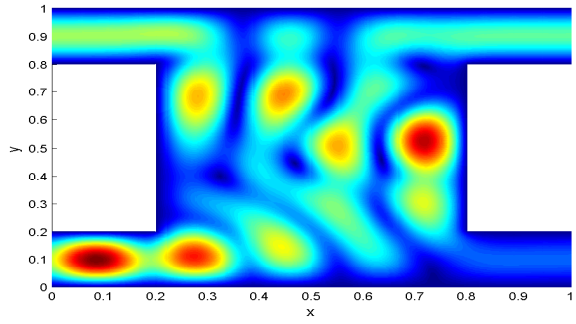

Figure 2: Example 1, the contour of the wave amplitude $|\varphi(x, y)|$.

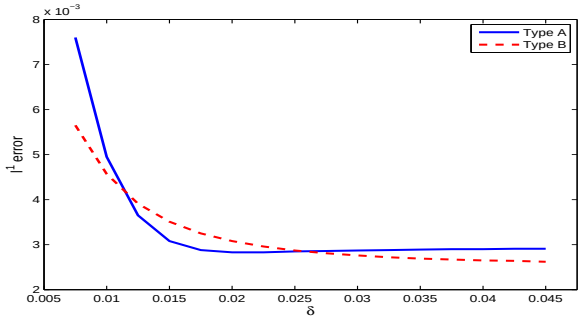

Figure 3: Example 1, the error reducing factor as a function of δ. Here $h = 1/400$.

h	$\frac{1}{100}$	$\frac{1}{200}$	$\frac{1}{400}$	$\frac{1}{800}$
Type A	3.51×10^{-1}	7.16×10^{-2}	1.54×10^{-2}	2.98×10^{-3}
ratio	$---$	4.90	4.65	5.17
Type B	3.14×10^{-1}	5.95×10^{-2}	1.32×10^{-2}	3.39×10^{-3}
ratio	$---$	5.28	4.51	3.89

Table 3: Example 2, the l^1 errors of wave functions for different mesh sizes and discrete interface conditions. The fourth group of coefficients is used.

	$h = \frac{1}{400}$		$h = \frac{1}{800}$	
	CPU time	l^1 error	CPU time	l^1 error
Type A	0.72s	1.54×10^{-2}	1.95s	2.98×10^{-3}
Type B	0.91s	1.32×10^{-2}	2.13s	3.39×10^{-3}
Finite difference	4.71s	1.97×10^{-2}	28.52s	4.02×10^{-3}

Table 4: Example 2, comparisons of the domain and subband decomposition method and the finite difference method. The fourth group of coefficients is used.

The simulation is done under

$$N_p = 16 \ (p = 1, 2, 3, 4), \ N_5 = 40, \ \text{ and } \ \delta = 1/80.$$

In Figure 4, we plot the contour of the wave amplitude $|\varphi(x, y)|$ with various coefficients of incoming waves in (2.6)-(2.7):

(1) $a_2^1 = 1, \quad a_n^p = 0(\text{others}),$

(2) $a_2^1 = a_1^2 = 1, \quad a_n^p = 0(\text{others}),$

(3) $a_2^1 = a_1^2 = a_1^3 = 1, \quad a_n^p = 0(\text{others}),$

(4) $a_2^1 = a_1^2 = a_1^3 = a_1^4 = 1, \quad a_n^p = 0(\text{others}).$

From the figure, we can see different interference phenomenon.

We output the l^1 errors of wave functions for different mesh sizes h and different discrete interface conditions in Table 3. In Table 4, the computational time and the l^1 error for the finite difference method and the domain and subband decomposition method are also compared. From all these tables, we can draw the same conclusion as in Example 1.

Example 3. We consider the two dimensional Schrödinger equation with

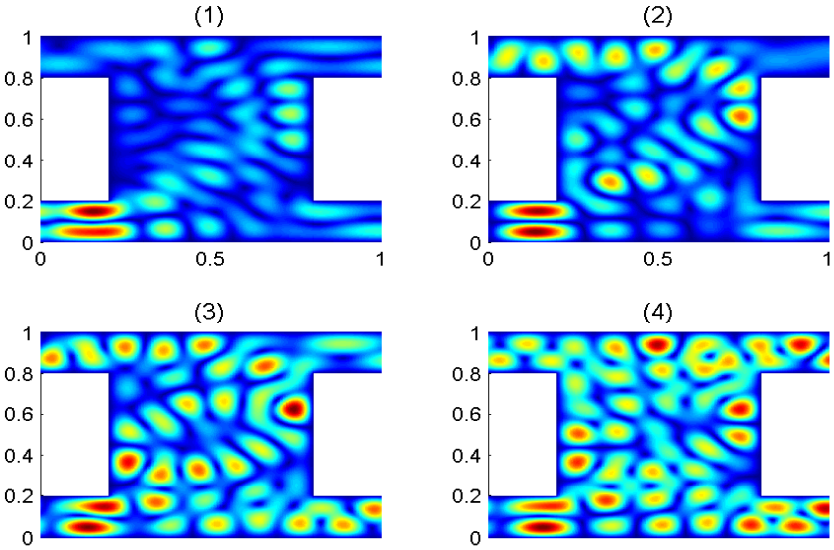

Figure 4: Example 2, the contour of the wave amplitude $|\varphi(x,y)|$ with various coefficients of incoming waves.

the following parameters

$$l_1 = h_1 = 0.2,\ l_2 = h_2 = 0.6,\ E = 0.6,\ \varepsilon = 0.05,$$
$$V(x,y) = e^{-100(x-0.5)^2-36(y-0.5)^2},\ (x,y) \in \Omega,$$
$$a_n^p = \begin{cases} 1, & n = p = 1, \\ 0, & \text{else.} \end{cases}$$

The simulation is done under

$$N_p = 16\ (p = 1,2,3,4),\ N_5 = 40, \quad \text{and} \quad \delta = 1/80.$$

In this example, the external potential varies in horizontal direction. Thus the coefficients $c_{nm}^{p1}(x)$ and $c_{nm}^{p2}(x)$ is non-zero for $n \neq m$.

In Figure 5, the contour of the external potential $V(x,y)$ and the wave amplitude $|\varphi(x,y)|$ are plotted. We output the l^1 errors of wave functions for different mesh sizes h and different discrete interface conditions in Table 5. In Table 6, the computational time and the l^1 error for the finite difference method and the domain and subband decomposition method are also compared. From all these tables, we can draw the same conclusion as in Example 1.

h	$\frac{1}{100}$	$\frac{1}{200}$	$\frac{1}{400}$	$\frac{1}{800}$
Type A	1.53×10^{-1}	1.52×10^{-2}	2.66×10^{-3}	6.11×10^{-4}
ratio	$---$	10.1	5.71	4.35
Type B	1.12×10^{-1}	2.03×10^{-2}	3.01×10^{-3}	5.89×10^{-4}
ratio	$---$	5.52	6.74	5.11

Table 5: Example 3, the l^1 errors of wave functions for different mesh sizes and discrete interface conditions.

	$h = \frac{1}{400}$		$h = \frac{1}{800}$	
	CPU time	l^1 error	CPU time	l^1 error
Type A	0.61s	2.66×10^{-3}	2.67s	6.11×10^{-4}
Type B	0.82s	3.01×10^{-3}	3.20s	5.89×10^{-4}
Finite difference	4.71s	2.30×10^{-3}	27.36s	5.48×10^{-4}

Table 6: Example 3, comparisons of the domain and subband decomposition method and the finite difference method.

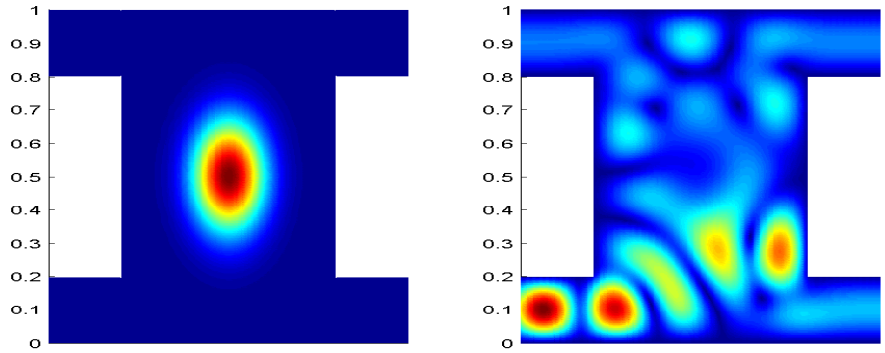

Figure 5: Example 3. Left: the contour of the external potential $V(x, y)$; right: the contour of the wave amplitude $\varphi(x, y)$.

4 Conclusion

Since the direct subband decomposition method is not applicable to the 2D Schrödinger equation on complicated geometrical domain, we propose a domain decomposition technical. The finite difference method is used in small irregular sub-domains, instead of the subband decomposition method. The interface conditions are given to connect two numerical methods. Through several numerical examples, we show the efficiency and accuracy of this method.

It will be of interest to study the method in the full three space dimensions and for the dynamic problems, which will be the subject of our future study. The other interesting topic is to analyze the stability and the convergence rate of the numerical scheme. It is still under investigation.

Acknowledgement

I am grateful to Z.Y. Huang and F. Méhats for helpful discussions.

References

[1] N. Ben Abdallah, *On a multidimensional Schrödinger-Poisson scattering model for semiconductors*, Joural of Mathematical Physics, 41(2000), no. 7, 4241-4261.

[2] N. Ben Abdallah, C. Negulescu, M. Mouis and E. Polizzi, *Simulation Schemes in 2D Nanoscale MOSFETs: A WKB Based Method*, Journal of Computational Electronics 3(2004), 397C400.

[3] Y. Achdou and Y. Maday, *The mortar element method with overlapping subdomains*, SIAM Journal on Numerical Analysis, 40(2002), no. 2, 601-628.

[4] J.A. del Alamo and C.C. Eugster, *Quantum field-effect directional coupler*, Applied Physics Letters, 56(1990), no. 1, 78-80.

[5] W.Z. Bao, S. Jin and P.A. Markowich, *On time-splitting spectral approximations for the Schrödinger equation in the semiclassical regime*, Journal of Computational Physics, 175(2002), 487-524.

[6] W.Z. Bao, S. Jin and P.A. Markowich, *Numerical studies of time-splitting spectral discretizations of nonlinear Schrödinger equations in the semiclassical regime*, SIAM Journal on Scientific Computing, 25(2003), no. 1, 27-64.

[7] L. Burgnies, O. Vanbésien and D. Lippens, *Transient analysis of ballistic transport in stublike quantum waveguides*, Applied Physics Letters, 71(1997), no. 6, 803-805.

[8] M. Büttiker, Y. Imry, R. Landauer and S. Pinhas, *Generalized many-channel conductance formula with application to small rings*, Physical Review B, 31(1985), no. 10, 6207-6215.

[9] P. Degond and S. Jin, *A smooth transition model between kinetic and diffusion equations*, SIAM Journal on Numerical Analysis, 42(2005), 2671 - 2687.

[10] P. Degond, S. Jin and L. Mieussens, *A smooth transition model between kinetic and hydrodynamic equations*, Journal of Computational Physics, 209(2005), 665-694.

[11] C.C. Eugster and J.A. del Alamo, *Tunneling Spectroscopy of an Electron Waveguide*, Physical Review Letters, 67(1991), no. 25, 3586-3589.

[12] F. Golse, S. Jin and C.D. Levermore, *A Domain Decomposition Analysis for a Two-Scale Linear Transport Problem*, Mathematical Modelling and Numerical Analysis, 37(2003), no. 6, 869-892.

[13] Y.Q. Huang and J.C. Xu, *A conforming finite element method for overlapping and nonmatching grids*, Mathematics of Computation, 72(2003), no. 243, 1057-1066.

[14] S. Jin, P. Markowich and C. Sparber, *Mathematical and computational methods for semiclassical Schrödinger equations*, Acta Numerica, 20(2011), 121-209.

[15] A. Klar, *Asymptotic-induced Domain Decomposition methods for Kinetic and Drift Diffusion Semiconductor equations*, SIAM Journal on Scientific Computing, 19(1998), no. 6, 2032-2050.

[16] C. Lent and D. Kirkner, *The quantum transmitting boundary method*, J. Appl. Phys., 67(1990), 6353-6359.

[17] T. Palm and L. Thylén, *Design logic functions using an electron waveguide Y-branch swith*, Journal of Applied Physics, 79(1996), no. 10, 8076-8081.

[18] E. Polizzi and N. Ben Abdallah, *Self-consistent three dimensional models for quantum ballistic transport in open system*, Physical Review B, 66(2002), 245301.

[19] E. Polizzi and N. Ben Abdallah, *Subband decomposition approach for the simulation of quantum electron transport in nanostructures*, Journal of Computational Physics, 202(2005), 150-180.

[20] E. Polizzi, N. Ben Abdallah, O. Vanbésien and D. Lippens, *Space lateraltransfer and negative differential conductance regimes in quantum wave guide junctions*, Journal of Applied Physics, 87(2000), no. 12, 8700-8706.

[21] A. Toselli, *HP-finite element approximations on non-matching grids for partial differential equations with non-negative characteristic form*, Mathematical Modelling and Numerical Analysis, 37(2003), no. 1, 91-115.

[22] W.D. Sheng, *Quantum coherent networks: A theoretical study*, Journal of Applied Physics, 81(1997), no. 9, 6210-6213.

[23] F. Sols, M. Maccuci, U. Ravaioli and K. Hess, *Theory for a quantum modulated transistor*, Journal of Applied Physics, 66(1989), no. 8, 3892-3906.

[24] A. Toselli and O. Widlund, *Domain Decomposition Methods - Algorithms and Theory*, Springer-Verlag Berlin, 2005.

[25] P.A. Markowich, P. Pietra and C. Pohl, *Numerical approximation of quadratic obaservables of Schrödinger-type equations in the semiclassical limit*, Numerische Mathematik, 81(1999), no. 4, 595-630.

[26] P.A. Markowich, P. Pietra, C. Pohl and H.P. Stimming, *A wigner-measure analysis of the Dufort-Frankel scheme for the Schrödinger equation*, SIAM Journal on Numerical Analysis, 40(2002), no. 4, 1281-1310.

[27] Jinchao Xu, *Iterative methods by space decomposition and subspace correctioon*, SIAM Review, 34(1992), no. 4, 581-613.

[28] Jinchao Xu and Jun Zou, *Some nonoverlapping domain decomposition methods*, SIAM Review, 40(1998), no. 4, 857-914.